

Electrocatalytic activity of Ce-PbO₂/C anode for acid red B reduction in aqueous solution

Xiang Hu · Yang Yu · Lijuan Yang

Received: 9 August 2014 / Revised: 3 February 2015 / Accepted: 7 February 2015 / Published online: 19 February 2015
© Springer-Verlag Berlin Heidelberg 2015

Abstract Graphite–lead dioxide electrodes doped with rare earth Cerium (Ce-PbO₂/C electrodes) were prepared by electrodeposition. The scanning electron microscope results showed that the microstructure and crystal orientation of electrode surface were changed by Cerium doping. CeO₂ was detected from modified electrodes by X-ray diffraction analysis. The cyclic voltammetry spectra indicated that the oxidation peak potential of cerium-doped electrode was smaller than pure PbO₂ electrode. Effects of the novel electrode on acid red B degradation were evaluated systematically under different parameters, including applied voltage, initial pH, supporting electrolyte concentration, electrode spacing, and influent concentration. The results indicated that chemical oxygen demand, decolorization, and ammonia nitrogen removal rate of Ce-PbO₂/C electrodes reached 90.17, 99.98, and 97.23 %, respectively, after 60-min electrolysis at initial 1000 mg L⁻¹ acid red B concentration. The possible mechanism of acid red B degradation over Ce-PbO₂/C electrodes was monitored by gas chromatography-mass spectrometer.

Keywords Electrochemical oxidation · Ce-PbO₂/C electrode · Acid red B · GC-MS

Introduction

Azo dye is a typical pollutant in textile industry, food colorants, printing, and cosmetics manufacturing [1]. Acid red B (ARB) is one widely used dye for fiber, silk, nylon, wool, and

leather [2]. The composition of dye wastewater is complicated, including high COD, high pH range, and biological toxicity [3]. Azo dyes have azo groups and aromatic rings with sulfonate groups. The structure of dyes determines their color and poor biodegradability. Dyes would weaken photosynthesis, which is mortal for a large number of aquatic plants. The toxicity of azo dyes and their intermediates would break the balance of ecological system [4]. Phenols are the intermediates affecting the growth and reproduction of aquatic creatures.

Traditional degradation methods are coagulation, adsorption, biodegradation, and chemical degradation. However, both coagulation and adsorption are ineffective and will generate large amounts of sludge and waste which cannot satisfy the discharge standards. Therefore, further treatments for disposal are needed [5–7].

As dyes are stable under sunlight and resistance to microbial attack, they may be toxic to the microorganisms and are not affected by biodegradation [8].

It is necessary to find effective technologies to treat dye wastewater. Electrochemical oxidation has been proved highly efficient, cost saving, and simple in degrading complex compounds [9–11]. The most important merit is that it is friendly to the environment, because it does not need any other reagents. The anode materials determine the removal of dye and COD. PbO₂ is used widely in industry wastewater treatment because of its high stability, electrical conductivity, and easy availability [12]. PbO₂ can be prepared by electrodeposition in acidic and alkaline solution containing Pb²⁺.

Recently, a lot of research studies on doping species in the deposition bath were reported, including F [13], Ni, Fe [14], Co [15], Bi [16, 17], and rare earth elements. The results showed that doping species could change the characteristics of PbO₂ electrode, including catalytic activity and oxygen evolution potential. Recently, there were many studies on doping of rare earth, such as La₂O₃ and Er₂O₃ [18, 19], which can

X. Hu (✉) · Y. Yu · L. Yang
College of Chemical Engineering, Beijing University of Chemical Technology, Beijing 100029, People's Republic of China
e-mail: huxiang@mail.buct.edu.cn

X. Hu
e-mail: huxiang99@163.com

distract internal stress of PbO_2 to enhance the stability of electrode and achieve high removal efficiency [20]. Cerium and its oxide have been widely used in oxidation catalyst as they have strong oxidation ability [21].

In this work, graphite–lead dioxide electrodes doped with rare earth Cerium were prepared by electrodeposition. The characteristics of the novel electrode were investigated by SEM, XRD, and CV. ARB was selected as the model target. The effects of different parameters on ARB degradation on the novel electrode were evaluated systematically, such as applied voltage, initial pH, supporting electrolyte concentration, inter-electrode spacing, and influent concentration. Gas chromatography-mass spectrometer (GC-MS) spectra of ARB solution were recorded to investigate the removal process of ARB.

Experimental

Materials and instruments

The Ce- PbO_2/C electrodes were prepared by electrodeposition. First, $\alpha\text{-PbO}_2$ was formed in the alkaline solution consisting of NaOH and PbO. The $\alpha\text{-PbO}_2/\text{C}$ as anode was placed in the acid solution consisting of $\text{Pb}(\text{NO}_3)_2$, NaOH, NaF, $\text{Cu}(\text{NO}_3)_2$, HNO_3 , and $\text{Ce}(\text{SO}_4)_2$ to form Ce- PbO_2 . All other chemicals used for the experiments were analytical grade.

The surface morphologies of electrodes were studied by SEM (S-4700) and XRD (D/Max 2500 VB2+/PC). The thicknesses of layers were measured by Thickness Meter (PD-CT2). The removal of color and COD was tested by UV-2000 and COD digestion apparatus (HACH). The intermediate products of ARB degradation were detected by GC7890/MS5975.

The electrolytic cell was a cylindrical beaker whose capacity was 250 mL. There was 130-mL solution that contained ARB and sodium sulfate in the electrolytic cell.

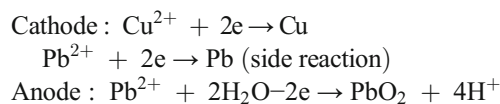
Electrode preparations

Graphite substrate was polished by sandpaper to reduce the edge effects. Then, the polished graphite was soaked in the solution of 2 mol L^{-1} NaOH for 1 h under $70\text{--}80^\circ\text{C}$, then in 1 mol L^{-1} HNO_3 for 20 min, and finally washed with distilled water.

The anode preparation procedures included $\alpha\text{-PbO}_2$ preliminary deposition and $\beta\text{-PbO}_2$ deposition. Lead oxide includes $\alpha\text{-PbO}_2$ and $\beta\text{-PbO}_2$. Two kinds of lead dioxide vary considerably, and the function in electrochemistry is also different. $\alpha\text{-PbO}_2$ is the skeleton of the active substance, and its electrical charge capacity is relatively small. $\beta\text{-PbO}_2$ which has higher electrical charge capacity clings to the skeleton

composed of $\alpha\text{-PbO}_2$. $\alpha\text{-PbO}_2$ has high structural strength and low discharge capacity. On the contrary, $\beta\text{-PbO}_2$ has low structural strength and high discharge capacity. The discharge capacity of $\beta\text{-PbO}_2$ is 1.5–3 times as great as $\alpha\text{-PbO}_2$, while $\alpha\text{-PbO}_2$ has good mechanical strength. The positive plate active material should not soften and exfoliate with the existence of $\alpha\text{-PbO}_2$. So, $\alpha\text{-PbO}_2$ needs to be electrodeposited firstly [22].

The $\alpha\text{-PbO}_2$ was formed in the solution consisting of PbO and NaOH (3.5 mol L^{-1}) for 1 h. The current density was 60 mA cm^{-2} , and the temperature was 40°C . Then, $\beta\text{-PbO}_2$ was formed in the acid solution including $\text{Pb}(\text{NO}_3)_2$, CTAB, NaF, $\text{Cu}(\text{NO}_3)_2$, and HNO_3 . The current density was 50 mA cm^{-2} , the temperature was 45°C , and the time of the deposition is 3 h. It is important to emphasize that $\text{Cu}(\text{NO}_3)_2$ was essential. Electrodeposition of lead nitrate acid solution could be obtained in lead dioxide anode active layer, and its main component was $\beta\text{-PbO}_2$. Mechanism of electrodeposition was that Cu^{2+} of the electrodeposition bath reduction reaction in the cathode and Pb^{2+} occurs oxidation reaction in the anode. The chemical equation could be expressed as



The main purpose of adding copper nitrate in electrodeposition solution was that it could inhibit the precipitation of lead on the cathode. Last, Ce- PbO_2/C were formed in the acid solution including CTAB (0.05 mol L^{-1}), $\text{Ce}(\text{SO}_4)_2$ (0.05 mol L^{-1}), HNO_3 (0.2 mol L^{-1}). The current density was 60 mA cm^{-2} , and the temperature was 40°C .

Analysis

The removal of color was analyzed by measuring the absorbance at 514 nm, which is the maximum absorbance wavelength of ARB. COD was detected by the potassium dichromate oxidation method. The removal rate of COD, decolorization, and ammonia nitrogen was all calculated by the following formula [1]:

$$\eta = \frac{A_0 - A_t}{A_0} \times 100\% \quad (1)$$

in which A_0 is the initial absorbance, COD, or ammonia nitrogen of dye waster, and A_t is the absorbance, COD, or ammonia nitrogen of dye after the reaction time t .

The intermediates were monitored by GC7890/MS5975 with HP-5 capillary column. The sampling mouth temperature is 250°C . The oven temperature was initially 50°C , rising at

15 °C min⁻¹ to a final temperature of 250 °C, and kept for 20 min. The flow rate of He as the carrier gas was 1 mL min⁻¹, and 1- μ L sample was injected.

Result and discussion

Characterization of electrodes

SEM and XRD

Figure 1 shows the SEM micrographs of the modified PbO₂ and pure PbO₂ anode. Pure PbO₂ has an incompact structure, and the crystal facet contains slight crack and uneven surface. Its crystal size is larger than modified PbO₂. Compared with the pure PbO₂, the Ce-PbO₂ anode has a smaller crystal size and a very compact structure. It can be inferred from the results that Ce doping can increase specific surface area and the active points and improve oxidation ability of the modified electrode.

The XRD spectrums of Ce-PbO₂/C and PbO₂/C electrodes are shown in Fig. 2. PbO₂/C shows the characteristic reflections of β -PbO₂ at 25.38°, 31.95°, and 62.48° [23]. The strongest diffraction peak is (301) crystal plane. Cerium doping weakens the intensity of β -PbO₂ and broadens the diffraction peak at 62.48°. The results show that Cerium doping diminishes the size of the crystal particles. At the same time, new diffraction peaks appeared at 29° and fit well with the diffraction peak of CeO₂ [18]. Above all, Cerium was enriched to the modified electrode surface, which greatly increased the contact area of the active substance and organic pollutants, and improved the catalytic performance of the electrode. The result of XRD is consistent with the SEM analysis.

The thicknesses of layers were also measured. The test result indicates that the thicknesses of layers were 200 μ m.

Cyclic voltammetry

A three-electrode system was used to conduct cyclic voltammetry. The reference electrode was saturated calomel electrode

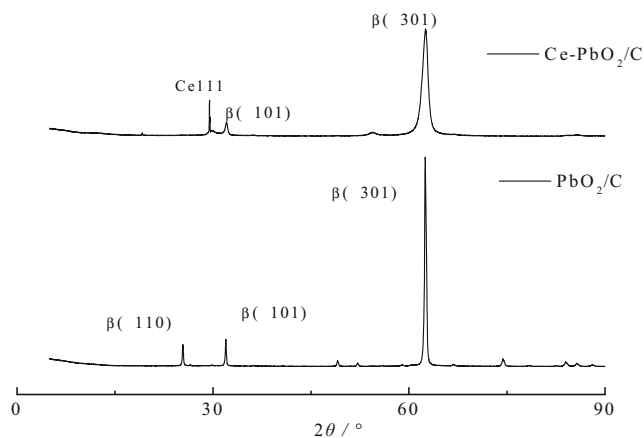


Fig. 2 XRD spectra of PbO₂/C and Ce-PbO₂/C electrode

(SCE). The counter electrode was platinum wire electrode (Pt). The working electrodes were Ce-PbO₂/C and PbO₂/C, respectively. The scan rate was 50 mV S⁻¹, and the dye concentration was 100 mg L⁻¹. The electrolytic cell was also a cylindrical beaker. Its capacity was 250 mL. The cyclic voltammograms are shown in Fig. 3, in which the dash line represents Ce-PbO₂/C and the solid line represents PbO₂/C.

Figure 3a shows that both Ce-PbO₂/C electrode and PbO₂/C electrode had apparent oxidation peaks. The oxidation current was also high. The system of H₂SO₄ had no obvious oxidation peak. This indicated that ARB could be directly oxidized at the electrode surface in alkaline and neutral system. However, in acid system, contaminants were hardly oxidized directly. Its degradation was mainly through the reaction with reactive groups of the solution-indirect oxidation [24]. Thus, alkaline and neutral systems are favorable for the degradation of ARB if the effects of electrolyte are omitted.

The cyclic voltammograms of Ce-PbO₂/C and PbO₂/C electrode in NaOH and Na₂SO₄ solution are shown in Fig. 3b. The blue lines represent NaOH system, while the red lines represent Na₂SO₄ system.

In Na₂SO₄ system, Ce-PbO₂/C electrode has two oxidation peaks, $E_p=0.698$ and 1.143 V, and the corresponding current peaks are $i_p=1.217 e^{-2}$ A and 1.974 e⁻² A. The potential and oxidative peak current of PbO₂/C electrode is 0.762 V and

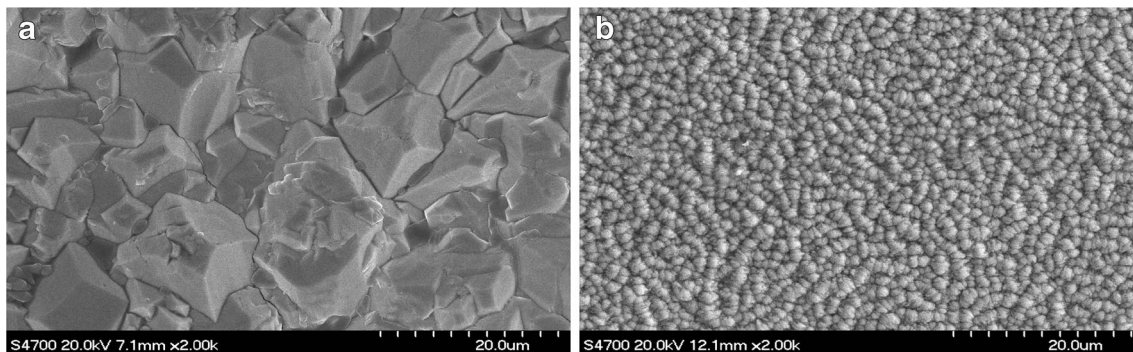


Fig. 1 SEM of PbO₂/C (a) and Ce-PbO₂/C (b) electrode

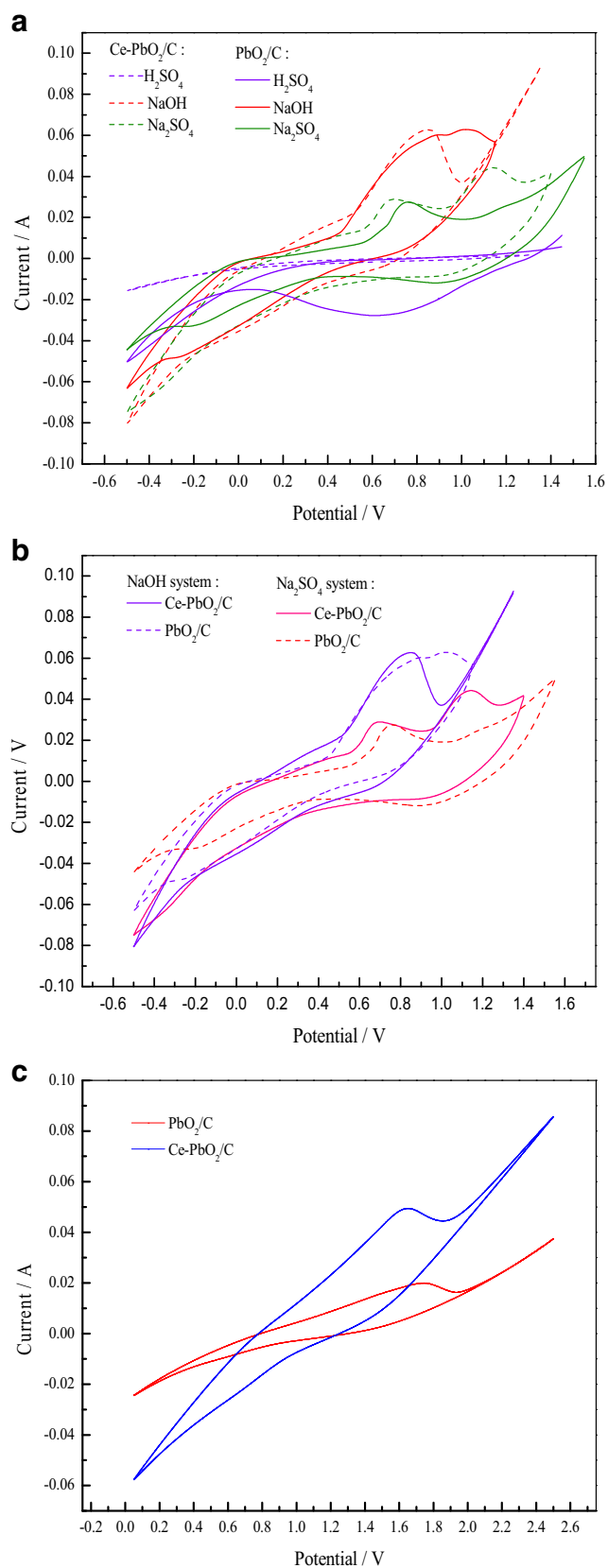


Fig. 3 CV of Ce-PbO₂/C and PbO₂/C electrode under **a** different conditions (H₂SO₄, NaOH, Na₂SO₄), **b** alkaline and neutral condition, and **c** acetic acid-sodium acetate buffer solution

1.581 e⁻² A. It is clearly seen that the oxidation potential of cerium-doped electrode diminishes, while the peak current becomes large. It can rapidly degrade organic contaminants because the speed and quantity of active matrix that the electrodes generate have increased [25]. In the catalytic oxidation process, when the current of oxidation peak or reduction peak was larger, the electrode surface is more uniform and dense, which is better for catalytic performance. It can provide more active sites to improve the catalytic ability of electrode in reaction [26, 27]. In NaOH system, the oxidation potential of cerium-modified electrode is small. This indicates that the oxidation peak of cerium-doped electrodes undergone some positive movement and dyes are more susceptible to oxidation.

The cyclic voltammograms for PbO₂/C electrode and Ce-PbO₂/C electrode in acetic acid-sodium acetate buffer solution are shown in Fig. 3c. Red line and blue line indicated the cyclic voltammograms of PbO₂/C electrode and Ce-PbO₂/C electrode, respectively. It could be seen from the figure that both of the two curves appeared oxidation peak, but reduction peak was not visible. This phenomenon indicated that the electrolysis reaction of ARB was an irreversible reaction. In addition, we could see that the oxidation peak potential of PbO₂/C electrode was 1.746 V and the peak current is 1.997 e⁻² A. This result was similar to the conclusions of document 28 [28]. However, the Ce-doped electrode had lower oxidation peak potential and higher current. The peak potential shifted toward lower potential value and the peak current increased sharply. It suggested that ARB had a more sensitive electrochemical response in Ce-PbO₂/C electrode. So, the degradation efficiency of ARB was higher. It was also consistent with the results of single factor experimental. The reduction of the peak potential was advantageous to the reaction; meanwhile, it could restrain oxygen evolution reaction to some extent, which should further increase the degradation efficiency of ARB.

In addition, other buffer solutions such as phosphate buffer solution and carbonic acid-sodium carbonate buffer solution were also used for cyclic voltammetry. No oxidation peak was found in these solutions. Therefore, the acetic acid-sodium acetate buffer solution was selected as the supporting electrolyte of cyclic voltammetry.

Electrode stability

Electrode stability test

A basic condition of electrodes to achieve large-scale industrial application was the stability of the electrode. Oxygen generated from oxygen evolution reaction diffused into the surface of the substrate, and it would cause deactivation of the electrode. After prolonged use, the oxygen evolution reaction occurred frequently, and the ability to degrade organic matter declined. Figure 4 shows the treatment effect of

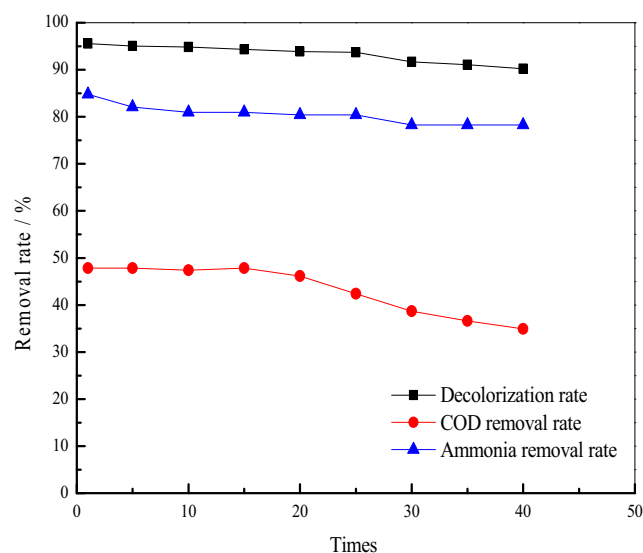


Fig. 4 The effect of the use of electrodes on treatment efficiency

electrode after continuous repeated use under the conditions that include that voltage was 10 V, pH was 7, the supporting electrolyte concentration was 4 g L^{-1} , the reaction time was 1 h. It indicated that the treatment efficiency of electrode was almost unchanged after working 1–15 times. The decolorization rate, ammonia removal rate, and COD removal rate decreased 1.64, 4.34, and 1.66 % after working 20 times. The treatment effect reduced slightly faster after working 20 times. The decolorization rate, ammonia removal rate, and COD removal rate decreased 5.33, 6.52, and 12.91 % after working 40 times compared with the first use of the electrode. Under the experimental conditions that voltage was 10 V, current density was selected between 200 and 500 mA cm^{-2} , and the removal rate achieved half of the original efficiency after working at least 70 times as the view of descending rate of 20 times to 40 times, according to the COD removal rate. Electrode surface was intact. It indicated that the electrode had good stability. The changes of before and after using electrode were compared by SEM and XRD. The reason that treatment efficiency reduced was revealed.

Characterization of used electrode

SEM Figure 5 shows the morphology and crystal of electrode surface by SEM analysis (before reaction (Fig. 5a), after reaction (Fig. 5b)). Magnification was $\times 5000$. Before using, the electrode surface was dense and crystal was symmetrical. However, it becomes rough and there were white spots on the grain, which were impurities. Grain surface was covered with a layer of film. The possible reason was acid corrosion, or oxygen evolution reaction occurs during the process of use. The roughness of electrode surface and the amount of contaminants increased. Thereby, the effective area of the electrode reduced. Therefore, the catalytic performance and treatment

efficiency of electrode reduced correspondingly. Judging from the results of the experiment, the significant reduction of decolorization, ammonia removal rate, and COD removal rate after 20 times reaction accorded with this rule. The oxidation reaction, oxygen evolution reaction, and acid corrosion led to the increase of electrode roughness when the time of using electrode increased [29]. Although adsorption of organic matter was more serious, the catalytic efficiency of organic matter reduced.

XRD Figure 6 shows XRD test of electrode used 40 times continuously. It was found that the peak position of the diffraction peaks does not change comparing with used electrode and unused electrode. Nevertheless, the peak intensity of the latter was weakened. After using, the width of 62° narrowed and it indicated that the particle size become large. Electrode diffraction peak appeared at 29.67° and 31.9° which are Ce (111) and β (101) before using. A slight change that the only diffraction peaks appeared at 31.92° after using. The reason why a small amount of the original CeO_2 crystals were decreasing as the electrode use time increased was that crystal particles could be cracked and damaged during the electrode use. Therefore, the characteristic diffraction peaks of Ce at 31.92° decreased. It mainly showed the diffraction peaks of β - PbO_2 . These results suggested that the relative intensity of each element weakened and the crystal form had not changed.

Effect of operating parameters

Effect of applied voltage

Voltage determines the electron transfer rate, affects the generation speed of active groups, and thus determines the degradation rate of organic materials. Electrolysis was conducted when the initial ARB concentration was 1 g L^{-1} , electrode spacing was 1.5 cm, pH was 6, and the supporting electrolyte concentration was 5 g L^{-1} . pH was adjusted by dilute H_2SO_4 and NaOH. Figure 7a shows the results of decolorization, COD, and ammonia nitrogen removal under different applied voltage after 1-h electrolysis. The decolorization rate increased from 60.75 to 99.98 %, as the applied voltage increased from 2 to 6 V, and the COD removal rate was increased by 52 % approximately. The removal efficiency of COD and ammonia nitrogen was greater than decolorization rate with the increase of applied voltage. When the applied voltage increases, the mass transfer, hydroxyl radical generation, electron transfer, and the adsorption and desorption of organics on the electrode were accelerated. These effects speeded up the ARB degradation. However, the decolorization rate and ammonia nitrogen removal rate remained nearly unchanged, while the COD removal rate continued to rise. The COD removal rate reached 86.00 % when the applied voltage increased to 10 V. Although the applied voltage

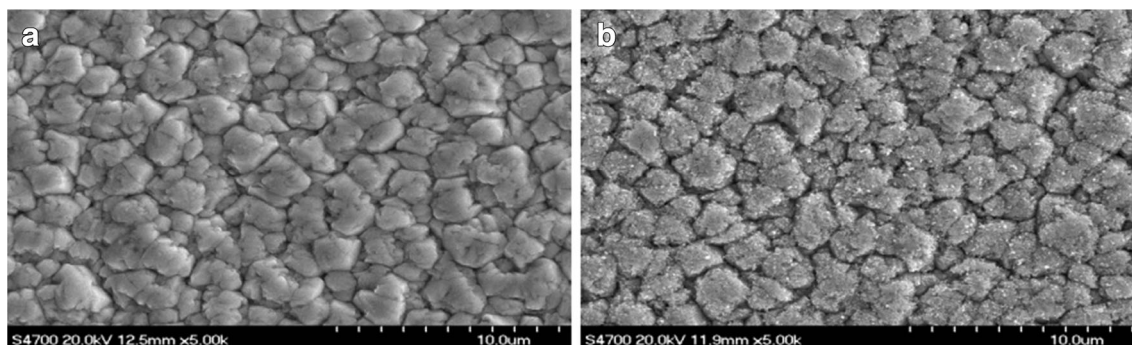


Fig. 5 Micrograph of the surface of Ce-PbO₂/C electrode (**a** before reaction and **b** after reaction)

influenced the mineralization of organic pollutants, hydrogen and oxygen evolution easily happened at higher voltage. This phenomenon hampers the formation, mass transfer, and diffusion of hydroxyl radicals, making the degradation of ARB no longer conspicuous at higher voltage. On the other hand, excessive voltage may also affect the stability and service life of electrodes [30]. As a result, the suitable applied voltage should be 10 V.

Effect of initial pH

pH values will affect the type of reactive groups in solution and influences conversion between HClO, Cl₂, and ClO⁻. These reactive groups will have a huge impact on degradation of ARB. Figure 7b shows that the influence of pH values ranged from 4 to 12 on decolorization, COD, and ammonia nitrogen removal. The remaining conditions remained unchanged except that the applied voltage was 10 V. The results indicate that the decolorization rate was above 99.00 % and stayed nearly unchanged regardless of the applied pH. The removal rate of ammonia nitrogen had the same phenomenon.

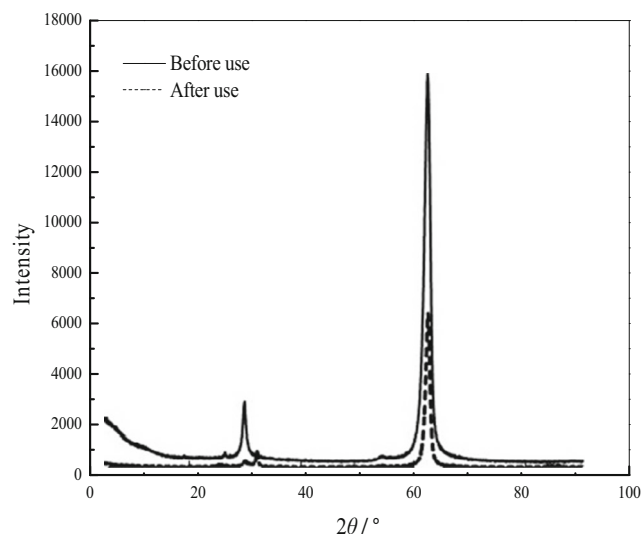


Fig. 6 XRD of Ce-PbO₂/C electrode that before and after used

However, COD was more easily influenced by pH. The removal of COD was above 83.00 % in the pH range of 4–8. The result was determined by different oxidizing ability of reactive species in different pH ranges. The majority of chlorine is in the form of HClO at pH ≥ 4 and when pH ≥ 6, they were converted to ClO⁻. At pH = 6, COD removal rate reached a maximum of 88.90 %. However, COD removal rate is only 68.57 % when pH is 12. Based on the experimental date, the degradation of COD would take place more rapidly in an acidic or neutral condition. There are two possible reasons. One is that pH affects the form of chlorine in solution. The chlorine is in the form of active Cl₂ when pH is 3. Chlorine evolution is apt to happen due to Cl₂ oxidation potential (1.36 V), which hinders the degradation of the dye molecules. The main specie of chlorine is HClO in pH range between 3 and 8. When pH is greater than 8, main form of chlorine is ClO⁻. As the oxidizing ability of HClO ($E^{\theta}=1.5$ V) is stronger than ClO⁻ ($E^{\theta}=0.89$ V), ARB is easy to mineralize in an acidic or neutral condition [31]. Another reason is that Na⁺ can combine with ClO⁻ to inhibit the oxidation of ARB [32]. So, the appropriate initial pH value ought to be 6.

Effect of supporting electrolyte concentration

Sodium chloride was selected as supporting electrolyte, which can improve the degradation efficiency and increase the formation of chlorine or hypochlorite during the electrolysis [33]. Effects of different supporting electrolyte concentration on the treatment effect are shown in Fig. 7c. The results show that removal rate of decolorization and ammonia nitrogen reached 99.97 and 97.23 %, respectively, when the supporting electrolyte concentration was 4 g L⁻¹. The decolorization rate nearly did not increase at higher supporting electrolyte concentration. However, it can be seen that COD removal rate continues to rise with the increase of supporting electrolyte concentration. The highest COD removal rate reached more than 90 % at the supporting electrolyte concentration of 6 g L⁻¹. The increased supporting electrolyte concentration not only enhanced conductivity but also strengthened the indirect oxidation ability due to higher concentration of Cl₂/HClO/ClO⁻ [34]. If the

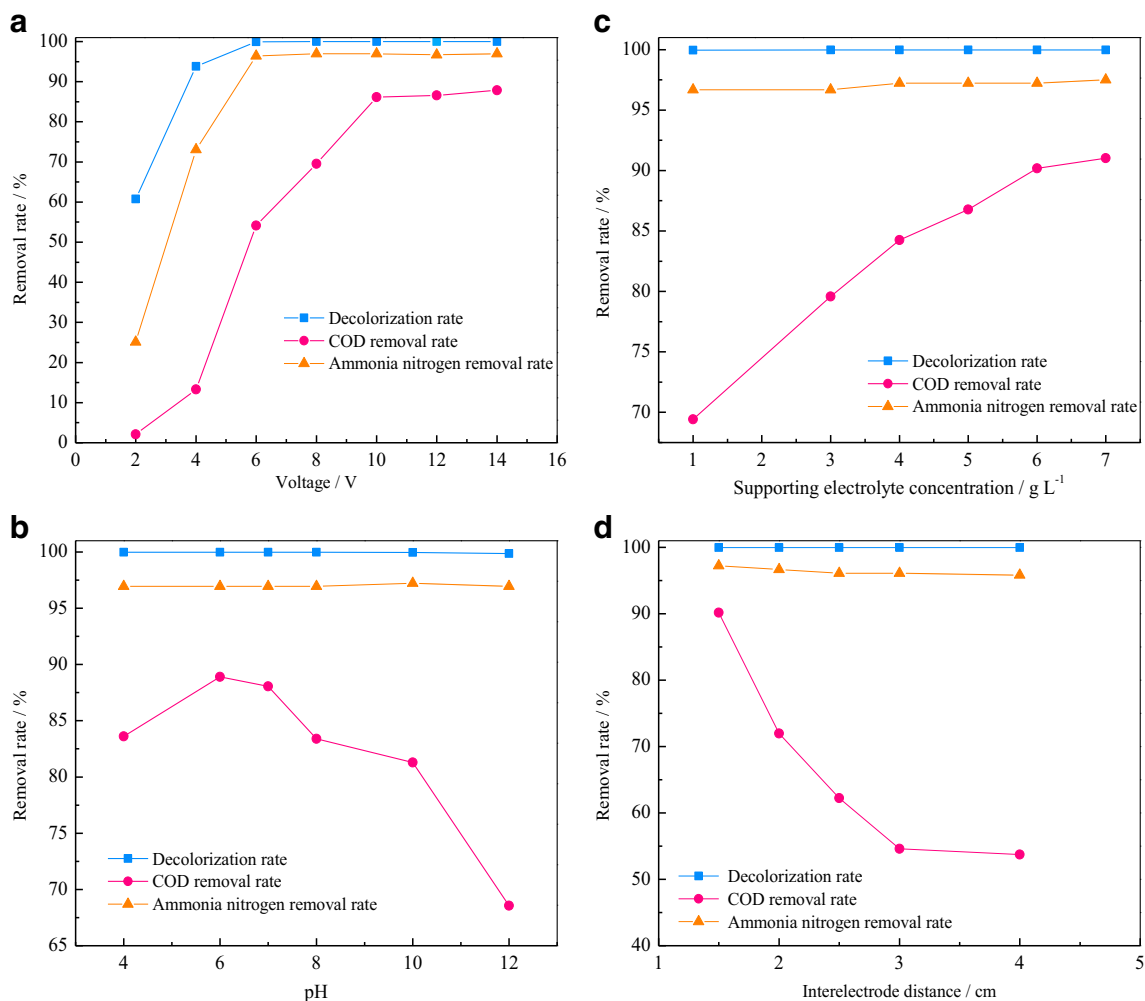


Fig. 7 Effect of **a** voltage, **b** pH, **c** supporting electrolyte concentration, and **d** interelectrode distance on the removal efficiency of color, COD, and ammonia nitrogen

supporting electrolyte concentration continued to increase, too much electrical energy will be converted to heat, and the temperature of the solution will be significantly increased. A higher removal rate is not expected; instead, a decline in the efficiency of the current would happen. Therefore, the suitable supporting electrolyte concentration is 6 g L⁻¹.

Effect of electrode spacing

Figure 7d shows the influence of different electrode spacing on the removal effect. It can be seen in Fig. 8 that smaller electrode spacing gave better removal rate. Decolorization rate decreased from 99.98 to 99.95 %, COD removal rate reduced from 90.17 to 53.75 %, and ammonia nitrogen removal rate was reduced by 1.4 %, as electrode spacing increases from 1.5 to 4 cm. The decolorization rate and COD removal rate decreased significantly when the electrode spacing varied from 1.5 to 3 cm. When the electrode spacing is greater than 3 cm, removal rate leveled off. Smaller electrode spacing decreased the electric resistance and enhanced the current, production of

reactive group, and oxidation capacity. When the electrode spacing is large, the decreased electron transfer rate would lead to the untimely degradation of intermediate products. They gradually deposited on the surface of electrode, causing contamination and decreased activity to the electrode. This phenomenon is harmful to the migration of contaminants on the electrode surface and the degradation effect [35]. However, larger electrode spacing increased the mass transfer resistance and thus inhibits the degradation process. As shown in Fig. 8, when electrode spacing is less than 1.5 cm, the processing efficiency may continue to rise. However, it is prone to short circuit when the electrode spacing is too small, besides, excessive current density will shorten the life of the electrode.

Effect of influent concentration

Dye concentration and COD in the industrial wastewater are not constant. Therefore, the research on influent concentration has a certain value on treatment effect.

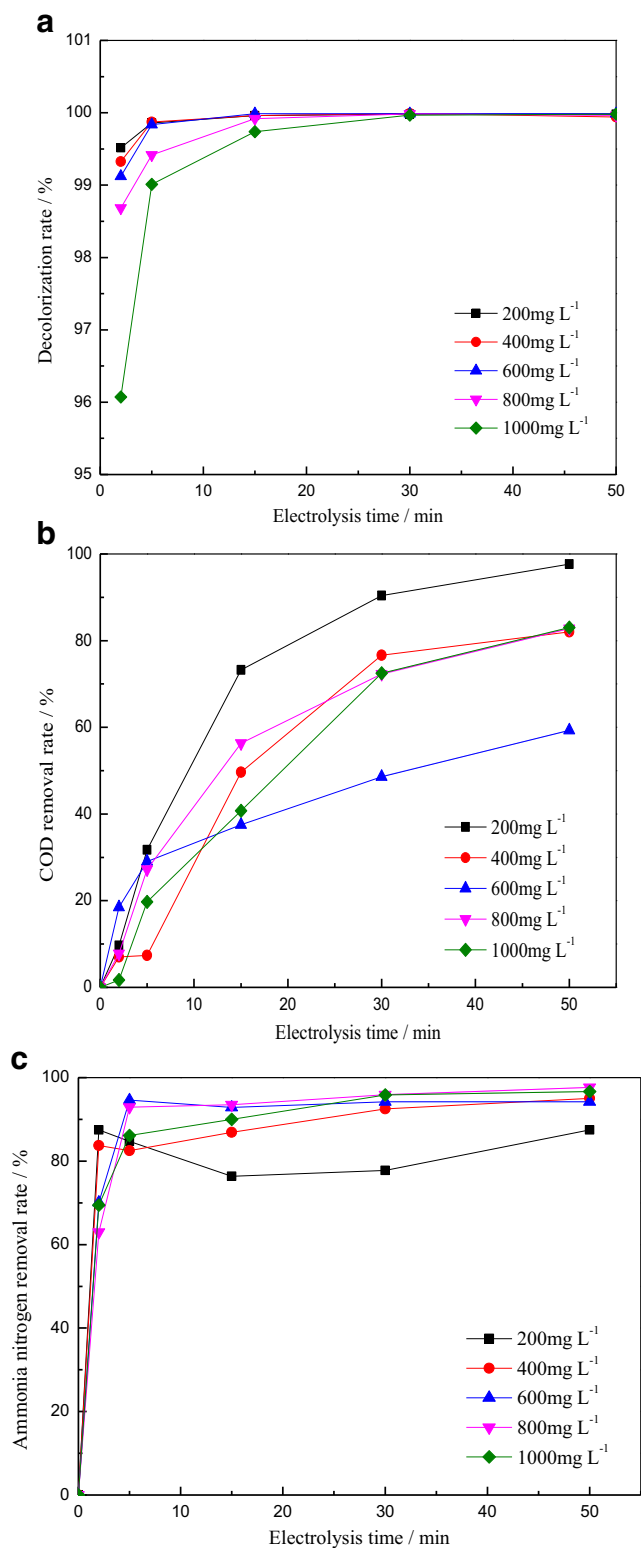


Fig. 8 The effect of the initial ARB concentration on **a** decolorization efficiency with time, **b** COD removal efficiency with time, **c** ammonia nitrogen removal efficiency with time (voltage 10 V, initial pH 6, supporting electrolyte (Na₂SO₄) concentration 6 g L⁻¹, interelectrode distance 1.5 cm)

Figure 8a shows the decolorization rate of different ARB concentration. The low concentration had high decolorization rate with reaction time ranging from 2 to 15 min. Outside this range, the decolorization rate was slow. After 5 min, the decolorization rate of 200 mg L⁻¹ influent concentration reached 99.85 %. When the influent concentration was 1 mg L⁻¹, the decolorization rate was 99.01 %. Decolorization rate showed a downward trend with the increase of concentration. The decolorization rate increased rapidly in low concentration and remained almost unchanged in high concentration. The decolorization rate of dye wastewater was almost 100 % after 30 min, regardless of the influent concentration.

Figure 8b shows that the COD removal rate changed with influent concentration. When the reaction time was 15 min, we observed that COD removal rate had a downward trend with increasing concentration. Assuming that organic contaminants were oxidized by hypochloric acid at the electrode surface, the above results can be explained by diffusion control theory. At low concentration, the electrochemical oxidation rate of dye is faster than its diffusion rate, and the intermediates produced by dye electrolysis are completely oxidized on the electrode surface. When the influent concentration increases, ARB and intermediate product are transferred to the electrode surface, but the restricted diffusion of hypochlorite could not effectively oxidize contaminants, making COD decrease [36]. Both COD removal rate and amount showed an increasing trend after 50 min, while COD removal amount increases at higher influent concentration. Therefore, under the same conditions, higher current efficiency can be obtained in the treatment of high concentration wastewater to save more energy.

Figure 8c indicates the relationship between ammonia nitrogen removal rate and influent concentration. Ammonia nitrogen removal rate reached a stable value after 50 min as influent concentration changed from low to high. When the influent concentration was greater than 200 mg L⁻¹, ammonia nitrogen removal rate was above 94 %. Moreover, it had reached more than 96 % at the

Table 1 The main degradation intermediates of ARB by GC-MS

Name of the substance	Molecular formula
Phthalic anhydride	C ₈ H ₄ O ₃
<i>o</i> -Phthalic acid	C ₈ H ₆ O ₄
Diethyl phthalate	C ₁₂ H ₁₄ O ₄
Hexadecanamide	C ₁₆ H ₃₃ NO
Methyl hexadecanoate	C ₁₇ H ₃₃ O ₂
Dodecanoic acid	C ₁₂ H ₂₄ O ₂
Myristic acid	C ₁₄ H ₂₈ O ₂
Palmitic acid	C ₁₆ H ₃₂ O ₂
Acetone	C ₃ H ₆ O
Oxalic acid	C ₆ H ₁₀ O ₄

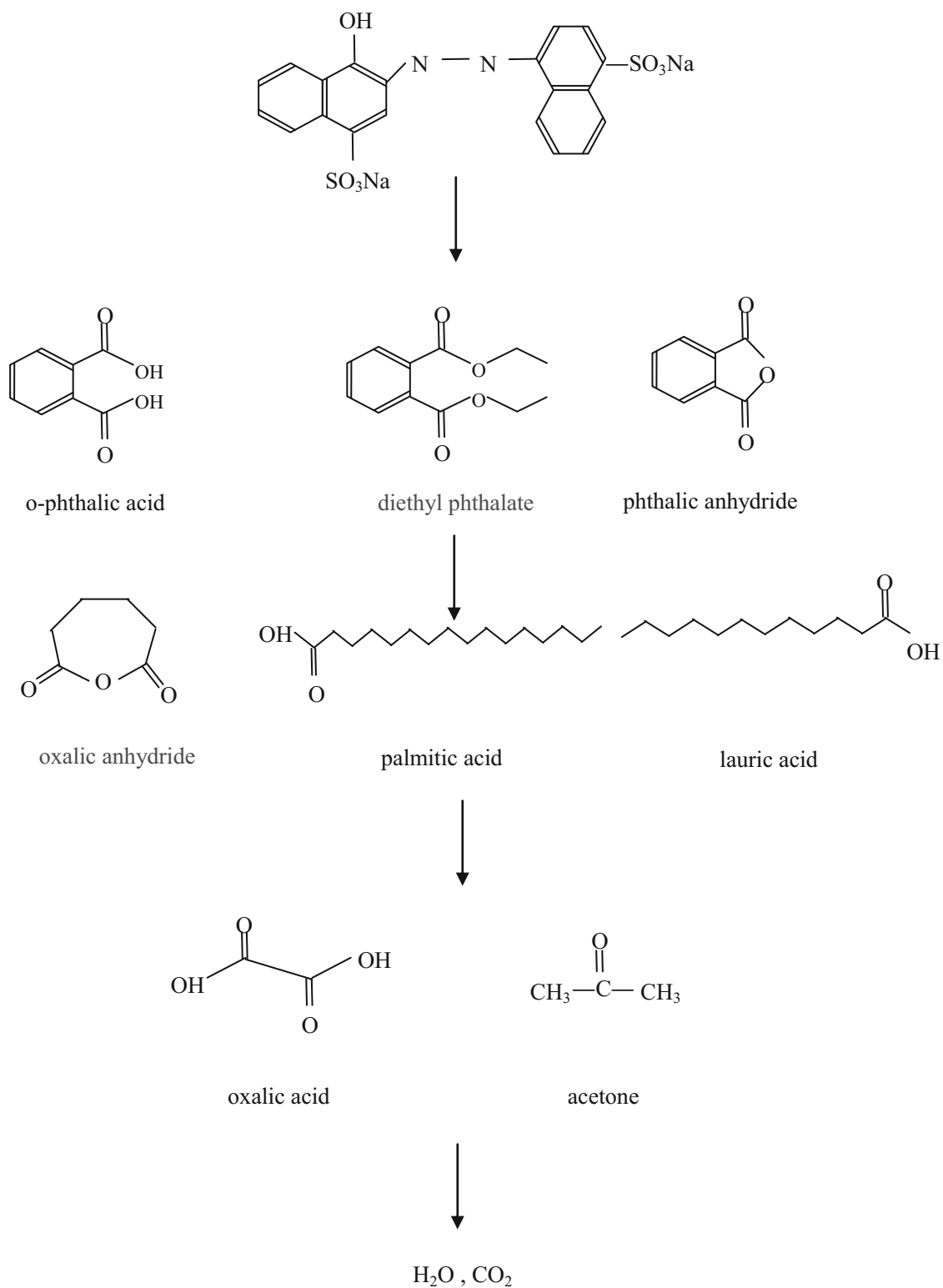


Fig. 9 A possible pathway for the degradation of ARB

concentration of 800–1000 mg L⁻¹. At the same time, ARB removal amount increases with the increase of initial ARB concentration. From the processing ability of pollutants and energy utilization rate, this method can be

applied to the treatment of high concentration dye wastewater.

Overall, when dealing with low concentration dye wastewater, higher energy and time efficiency can be obtained. The

reaction time may be extended or large applied voltage is needed to achieve the desired results in high concentration dye wastewater.

GC-MS analysis

GC-MS technique was applied to detect intermediates after electrolysis for 30 min. The technology is useful to analyze the degradation mechanism of dyes. The result in Table 1 showed that the structure of ARB was broken to form different intermediates, including phthalandione diethyl phthalate, and methyl hexadecanoate.

The break of azo bond would be the first step of dye degradation, which led to the rapid removal of color. The possible intermediates were A and B (hydrazo derivative). The sulfonic group in the hydrazo derivative was highly stable and soluble in solution [37]. A is easily degradable under aerobic condition. Therefore, it was not detected in the GC/MS analysis. As shown in Fig. 9, B was oxidized to some naphthalene-type intermediates or compounds containing benzene ring, such as phthalic anhydride, diethyl phthalate, and phthalic acid [38–40]. These intermediates were further oxidized to long-chain organic acids, e.g., palmitic acid and lauric acid. These compounds were further degraded to form oxalic acid and acetone. Finally, these small molecules were decomposed to CO_2 and H_2O .

The process of electrochemical oxidation of ARB was gradual. At first, ARB was degraded to aromatic intermediates, then oxidized to chain structure products and decomposed to CO_2 and H_2O at last.

Conclusions

A novel Ce-PbO₂/C electrode was prepared by electrodeposition. The SEM and XRD tests show that Ce doping in lead dioxide films can decrease the crystal size of anodes, increase their specific surface area, and improve the oxidation ability of the electrode. The cyclic voltammetry tests show that Ce-PbO₂/C electrodes had a wider oxidation peak and stronger capacity to generate reactive groups, and the oxidation peak potential of Ce-PbO₂/C electrode was smaller than pure PbO₂ electrode. Electrochemical removal of ARB in aqueous solution on Ce-PbO₂/C electrode was investigated to achieve desirable removal efficiency. The results show that the COD, decolorization, and ammonia nitrogen removal efficiency in 6 g L⁻¹ NaCl solution containing 1000 mg L⁻¹ ARB could achieve 90.17, 99.98, and 97.23 %, respectively, with an applied voltage of 10 V, pH value of 6, and electrode spacing of 1.5 cm after 50 min. Through the GC-MS analysis, ARB was firstly degraded to aromatic intermediates, then oxidized to chain structure products, and decomposed to CO_2 and H_2O .

Acknowledgments We thank the National Key Technology R&D Program of China (Project No. 2011BAE07B09-2) for financial support. Additionally, the analytical work was supported by the Water Pollution Control Laboratory of Beijing University of Chemical Technology.

References

- Zhou MH, He JJ (2008) Degradation of cationic red X-GRL by electrochemical oxidation on modified PbO₂ electrode. *J Hazard Mater* 153:357–363
- Wang J, Jiang Z, Zhang ZH, Xie YP, Wang XF, Xing ZQ, Xu R, Zhang XD (2008) Sonocatalytic degradation of acid red B and rhodamine B catalyzed by nano-sized ZnO powder under ultrasonic irradiation. *Ultrason Sonochem* 15:768–774
- Aquino JM, Pereira GF, Rocha-Filho RC, Bocchi N, Biaggio SR (2011) Electrochemical degradation of a real textile effluent using boron-doped diamond or β -PbO₂ as anode. *J Hazard Mater* 192: 1275–1282
- Körbahti BK, Artut K, Geçgel C, Özer A (2011) Electrochemical decolorization of textile dyes and removal of metal ions from textile dye and metal ion binary mixtures. *Chem Eng J* 173:677–688
- Banat F, Al-Bastaki N (2004) Treating dye wastewater by an integrated process of adsorption using activated carbon and ultrafiltration. *Desalination* 170:69–75
- Gupta VK, Mittal A, Gajbe V (2005) Adsorption and desorption studies of a water soluble dye, Quinoline Yellow, using waste materials. *J Colloid Interface Sci* 284:89–98
- Anouzla A, Abrouki Y, Souabi S, Safi M, Rhalal H (2009) Colour and COD removal of disperse dye solution by a novel coagulant: application of statistical design for the optimization and regression analysis. *J Hazard Mater* 166:1302–1306
- Alaton IA, Insel G, Eremektar G, Babuna FG, Orhon D (2006) Effect of textile auxiliaries on the biodegradation of dyehouse effluent in activated sludge. *Chemosphere* 62:1549–1557
- Zhu XP, Ni JR, Wei JJ, Xing X, Li HN (2011) Destination of organic pollutants during electrochemical oxidation of biologically-pretreated dye wastewater using boron-doped diamond anode. *J Hazard Mater* 189:127–133
- Kariyajanavar P, Jogtappa N, Nayaka YA (2011) Studies on degradation of reactive textile dyes solution by electrochemical method. *J Hazard Mater* 190:952–961
- Sanroma'n MA, Pazos M, Cameselle C (2004) Optimisation of electrochemical decolourisation process of an azo dye, Methyl Orange. *J Chem Technol Biotechnol* 79:1349–1353
- Duan XY, Ma F, Yuan ZX, Chang LM, Jin XT (2013) Electrochemical degradation of phenol in aqueous solution using PbO₂ anode. *J Taiwan Inst Chem Eng* 44:95–102
- Velichenko AB, Devilliers D (2007) Electrodeposition of fluorine-doped lead dioxide. *J Fluor Chem* 128:269–276
- Andrade LS, Ruotolo LAM, Rocha-Filho RC, Bocchi N, Biaggio SR, Niesta J, Garcia-Garcia V, Montiel V (2007) On the performance of Fe and Fe, F doped Ti–Pt/PbO₂ electrodes in the electrooxidation of the Blue Reactive 19 dye in simulated textile wastewater. *Chemosphere* 66:2035–2043
- Velichenko AB, Amadelli R, Baranova EA, Girenko DV, Danilov FI (2002) Electrodeposition of Co-doped lead dioxide and its physico-chemical properties. *J Electroanal Chem* 527:56–64
- Borrás C, Laredo T, Mostany J, Scharifker BR (2004) Study of the oxidation of solutions of p-chlorophenol and p-nitrophenol on Bi-doped PbO₂ electrodes by UV-Vis and FTIR in situ spectroscopy. *Electrochim Acta* 49:641–648

17. Liu Y, Liu HL (2008) Comparative studies on the electrocatalytic properties of modified PbO_2 anodes. *Electrochim Acta* 53:5077–5083
18. Dai QZ, Shen H, Xia YJ, Chen JM (2012) Typical rare earth doped lead dioxide electrode: preparation and application. *Int J Electrochem Sci* 7:10054–10062
19. Wang Y, Shen ZY, Li Y, Niu JF (2010) Electrochemical properties of the erbium–chitosan–fluorine–modified PbO_2 electrode for the degradation of 2, 4-dichlorophenol in aqueous solution. *Chemosphere* 79:987–996
20. Kong JT, Shi SY, Kong LC, Zhu XP, Ni JR (2007) Preparation and characterization of PbO_2 electrodes doped with different rare earth oxides. *Electrochim Acta* 53:2048–2054
21. Ai SY, Gao MN, Zhang W, Wang QJ, Xie YF, Jin LT (2004) Preparation of Ce- PbO_2 modified electrode and its application in detection of anilines. *Talanta* 62:445–450
22. Petersson I, Ahlberg E, Berghult B (1998) Parameters influencing the ratio between electrochemically formed α - and β - PbO_2 . *J Power Sources* 76:98–105
23. Liu HL, Liu Y, Zhang C, Shen RS (2008) Electrocatalytic oxidation of nitrophenols in aqueous solution using modified PbO_2 electrodes. *J Appl Electrochem* 38:101–108
24. Koehne JE, Marsh M, Boakye A, Douglas B, Kim IY, Chang S, Jang D, Bennet KE, Kimble C, Andrews R, Meyyappan M, Lee KH (2011) Carbon nanofiber electrode array for electrochemical detection of dopamine using fast scan cyclic voltammetry. *Analyst* 136:1802–1805
25. Masek A, Zaborski M, Chrzescijanska E (2011) Electrooxidation of flavonoids at platinum electrode studied by cyclic voltammetry. *Food Chem* 127:699–704
26. Santos DMF, Sequeira CAC (2010) Cyclic voltammetry investigation of borohydride oxidation at a gold electrode. *Electrochim Acta* 55:6775–6781
27. Kariyajjanavar P, Narayana J, Nayaka YA, Umanaik M (2010) Electrochemical degradation and cyclic voltammetric studies of textile reactive azo dye cibacron navy WB. *Port Electrochim Acta* 28:265–277
28. Yu NF, Gao LJ, Zhao SH, Wang ZD (2009) Electrodeposited PbO_2 thin film as positive electrode in PbO_2/AC hybrid capacitor. *Electrochim Acta* 54:3835–3841
29. Tong SP, Ma CA, Feng H (2008) A novel PbO_2 electrode preparation and its application in organic degradation. *Electrochim Acta* 53:3002–3006
30. Alaton IA, Balcioglu IA, Bahnemann DW (2002) Advanced oxidation of a reactive dye bath effluent: comparison of O_3 , $\text{H}_2\text{O}_2/\text{UV-C}$ and $\text{TiO}_2/\text{UV-A}$ processes. *Water Res* 36:1143–1154
31. Mascia M, Vacca A, Polcaro AM, Palmas S, Ruiz JR, Pozzo AD (2010) Electrochemical treatment of phenolic waters in presence of chloride with boron-doped diamond (BDD) anodes: experimental study and mathematical model. *J Hazard Mater* 174:314–322
32. Mukimin A, Wijaya K, Kuncaka A (2012) Oxidation of removal brilliant blue R (RB.19) with in situ electro-generated active chlorine using Ti/ PbO_2 electrode. *Sep Purif Technol* 95:1–9
33. Rajkumar D, Song BJ, Kim JG (2007) Electrochemical degradation of Reactive Blue 19 in chloride medium for the treatment of textile dyeing wastewater with identification of intermediate compounds. *Dyes Pigments* 72:1–7
34. Shen ZM, Wu D, Yang J, Yuan T, Wang WH, Jia JP (2006) Methods to improve electrochemical treatment effect of dye wastewater. *J Hazard Mater* 131:90–97
35. Wang YQ, Gu B, Xu WL (2009) Electro-catalytic degradation of phenol on several metal-oxide anodes. *J Hazard Mater* 162:1159–1164
36. Song S, Fan JQ, He ZQ, Zhan LY, Liu ZW, Chen JM, Xu XH (2010) Electrochemical degradation of azo dye C.I. Reactive Red 195 by anodic oxidation on Ti/ SnO_2 -Sb/ PbO_2 electrodes. *Electrochim Acta* 55:3606–3613
37. Zhao HZ, Sun Y, Xu LN, Ni JR (2010) Removal of Acid Orange 7 in simulated wastewater using a three-dimensional electrode reactor: removal mechanisms and dye degradation pathway. *Chemosphere* 78:46–51
38. Zhao WR, Shi HX, Wang DH (2003) Kinetics of the reaction between ozone and cationic red X-GRL. *Chin J Chem Eng* 11:388–394
39. Martins MAM, Lima N, Silvestre AJD, Queiroz MJ (2003) Comparative studies of fungal degradation of single or mixed bioaccessible reactive azo dyes. *Chemosphere* 52:967–973
40. Siddique M, Farooq R, Khan ZM, Khan Z, Shaukat SF (2011) Enhanced decomposition of reactive blue 19 dye in ultrasound assisted electrochemical reactor. *Ultrason Sonochem* 18:190–196